EUROPEAN ORGANIZATION FOR NUCLEAR RESEARCH

CERN-EP/79-75
10 July 1979

MESON-PROTON LARGE-ANGLE ELASTIC SCATTERING AT 20 AND 30 GeV/c

CERN[1]-Annecy (LAPP)[2]-Genova[3]-Copenhagen[4]-Oslo[5]-
London (U.C.)[6] Collaboration

R. Almås[5], C. Baglin[2], R. Böck[1], K. Brobakken[5], L. Bugge[5], T. Buran[5], A. Buzzo[3], P. Carlson[1], L. Causton[6], C. Caverzasio[2], M. Coupland[6], D. Davis[6], J. Dines-Hansen[4], B.G. Duff[6], A. Eide[5], S. Ferroni[3], I. Gjerpe[5], V. Gracco[3], K. Guettler[6], J.P. Guillaud[2], J. Haldorsen[5], P. Helgaker[1], F.F. Heyman[6], D.C. Imrie[6], T. Jacobsen[5], E. Johansson[1], K. Kirsebom[5], O. Kofoed Hansen[4], S. Kooijman[6], R. Lowndes[6], A. Lundby[1], G.J. Lush[6], M. Macri[1], R. Møllerud[4], J. Myrheim[4], M. Poulet[2], L. Rossi[3], A. Santroni[3], B. Schistad[5], H. Schwartz[5], G. Skjevling[5], S.O. Sørensen[5], J. Tavernier[2], M. Yvert[2]

ABSTRACT

In an experiment at the CERN SPS we have measured elastic scattering at 20 and 30 GeV/c in the scattering angular range from 45° to 90° in the centre of mass. We present data on the $\pi^{\pm}p$, $K^{-}p$ differential cross-sections at 20 GeV/c, and on the $\pi^{-}p$ cross-section at 30 GeV/c.

For large angles in the centre of mass we find for $\pi^{-}p$ elastic scattering an s-dependence of the cross-section as s^{-n} with $n \sim 9.5$. At smaller angles we find $n \sim 8$.

The data are compared with the constituent interchange model. We find some discrepancies between the data and predictions made by this model when comparing $\pi^{+}p$, $\pi^{-}p$ and $K^{-}p$ elastic scattering.

Submitted to the
EPS International Conference on High-Energy Physics,
Geneva, 27 June - 4 July 1979.

Geneva - 25 June 1979

1. THE EXPERIMENT

Figure 1 shows the layout of the experiment. The incident K or p were detected by two differential Čerenkov counters.

The beam intensity ranged from 2×10^7 to 8×10^7 particles/sec. The intensity was counted in planes of narrow scintillation counters, and independently measured in an ionization chamber.

The scattered particles were detected by a system of scintillation hodoscopes, combined in fast logic to satisfy coplanarity and opening angle requirements.

Threshold Čerenkov counters were used in both arms of the experiment. The trajectories of outgoing particles were measured in multiwire proportional chambers in each arm downstream of and within the spectrometer magnet.

The acceptance of the experiment was optimized to cover the region in $\cos \theta_{cm}$ between -0.1 and 0.7.

2. THE RESULTS

The results presented in this paper correspond to the full statistics of our 20 GeV/c data, and about 80% of the statistics at 30 GeV/c.

As a check of the over-all normalization in this experiment we have measured the pp elastic scattering at 20 GeV/c simultaneously with our π^+p data. Within statistical errors of ±40% our cross-section agrees with earlier data at 19.3 and 21.3 GeV/c.

In all figures only the statistical errors are given. The error in the over-all normalization due to correction factors applied to our cross-section is smaller than the statistical error in each bin.

In Fig. 2 we show the $\pi^-p \to \pi^-p$ differential cross-section measured in this experiment at 20 and 30 GeV/c, as a function of $\cos \theta_{cm}$. Also plotted are data at 22.6 GeV/c [1], 9.7/9.8 GeV/c [2], and at 6.2 GeV/c [3].

We observe that the cross-section at 30 GeV/c has decreased by almost 4 orders of magnitude from the previously highest energy measured in the large-angle region.

As there is no overlap between our data at 20 GeV/c and the data at 22.6 GeV/c, we cannot compare these two measurements directly.

The drawn curves are predictions of the constituent interchange model[4] which will be discussed further below.

In Fig. 3 we show the $\pi^+p \to \pi^+p$ differential cross-section at 20 GeV/c from this experiment, compared with data at 10 GeV/c [5]. The cross-section has decreased by about 2 orders of magnitude between 10 and 20 GeV/c. We see from Figs. 2 and 3 that the π^-p cross-section is similar to the π^+p cross-section at 20 GeV/c.

In Fig. 4 we show our $K^-p \to K^-p$ cross-section at 20 GeV/c, compared to data at 6.2 GeV/c [3]. The cross-section has decreased by about 3 orders of magnitude between these two energies. The K^-p cross-section at 20 GeV/c is based on 4 event. The cross-section at $\cos\theta \sim 0.5$ is similar to the $\pi^\pm p$ cross-sections at this energy.

We have studied the energy dependence of the π^-p cross-section at fixed scattering angle in the centre of mass. According to dimensional counting rules, the differential cross-section at high energies and large angles should be given by

$$\frac{d\sigma}{dt} \sim s^{-n} f(\theta_{cm}) \ ,$$

where s is the centre-of-mass energy and θ_{cm} is the centre-of-mass scattering angle. For meson-nucleon scattering we should have n = 8.

We have used the data at 9.7/9.8, 20, and 30 GeV/c to fit the values of n for fixed values of $\cos\theta_{cm}$. This corresponds to a range in s of $19\ \text{GeV}^2 < s < 58\ \text{GeV}^2$. Except for the first bin at $\cos\theta_{cm} = 0.6$, the data are consistent with an s^{-n} dependence for fixed $\cos\theta_{cm}$. The results are shown in Fig. 5, where n is plotted as a function of $\cos\theta_{cm}$.

For $\cos\theta_{cm} < 0.4$ the data are compatible with scaling, with the value $n \sim 9.5$. For larger values of $\cos\theta_{cm}$ we find $n \sim 8$. A possible 30 % normalization error between 9.7/9.8 GeV/c and our data would give a shift in the slope of ±0.4, which is within the statistical errors on our points. Lower-energy data[6], with $16\ \text{GeV}^2 < s < 19\ \text{GeV}^2$, give a value of $n = 10.3 \pm 1.6$ at $\theta_{cm} = 80°$.

Comparing the K^-p cross-section at 6.2 GeV/c and 20 GeV/c for $\cos\theta_{cm} \sim 0.5$, we get n compatible with 8.

In π^+p elastic scattering we have no measurement of the cross-section above 20 GeV/c. With only data at 10 and 20 GeV/c we therefore make no detailed study of the s-dependence of the cross-section. But, as shown below in a comparison with the constituent interchange model, the data at 10 and 20 GeV/c seem consistent with an s^{-8} dependence.

We have compared our data with the constituent interchange model (CIM)[4]. In this framework the differential π^+p, π^-p, and K^-p cross-sections are given by

$$\frac{d\sigma}{dt}(\pi^+p \to \pi^+p) = \frac{\sigma_0}{s^8}\,\frac{(1+Z)}{(1-Z)^4}\,\left[4\alpha\,(1+Z)^{-2} + \beta\right]^2 ,$$

$$\frac{d\sigma}{dt}(\pi^-p \to \pi^-p) = \frac{\sigma_0}{s^8}\,\frac{(1+Z)}{(1-Z)^4}\,\left[4\beta\,(1+Z)^{-2} + \alpha\right]^2 , \qquad (1)$$

$$\frac{d\sigma}{dt}(K^-p \to K^-p) = \frac{\sigma_0}{s^8}\,\frac{(1+Z)}{(1-Z)^4}\,\alpha^2 ,$$

where $Z = \cos\theta_{cm}$.

The constants σ_0, α, and β are the same for π^+p, π^-p, K^+p, and K^-p elastic scattering. We chose $\alpha = 2$, $\beta = 1$, as in Gunion et al.[4].

We have fitted our π^+p data at 20 GeV/c with the form (1), which then determines the value of σ_0.

The result of the fit is shown by the drawn curve in Fig. 3.

With this same value of σ_0, we then scale to π^+p scattering at 10 GeV/c, to π^-p scattering at 6.2, 9.7/9.8, 20, and 30 GeV/c, and to K^-p scattering at 6.2 and 20 GeV/c.

Figure 3 shows that the CIM-predicted cross-sections at 10 GeV/c agree well with the data in the large-angle region.

In Fig. 2 we see that the CIM predictions at 20 and 30 GeV/c are a factor of 2 lower than the measured cross-sections for $0.7 < \cos\theta_{cm} < 0.5$. At larger scattering angles the data agree with the predicitons, but, as seen above, the cross-section here falls faster than s^{-8}.

At 9.7/9.8 GeV/c the CIM prediction falls clearly below the data.

In K^-p scattering, we see in Fig. 4 a large discrepancy between the CIM prediction and our cross-section at 20 GeV/c for $\cos \theta_{cm} \sim 0.5$, but our low statistics make the comparison uncertain.

* * *

REFERENCES

1. P. Cornillon et al., Phys. Rev. Lett. 30 (1973) 403.
2. D.P. Owen et al., Phys. Rev. 181 (1969) 1794.
3. T. Buran et al., Nucl. Phys. B111 (1976) 1.
4. J.F. Gunion et al., Phys. Rev. D 8 (1973) 287.
   D. Sivers et al., Phys. Reports 23C (1976) 1.
5. C. Baglin et al., Phys. Rev. Lett. 40 (1978) 425.
6. K.A. Jenkins et al., Phys. Rev. Lett. 40 (1978) 425.

Figure Captions

Fig. 1 : Experimental layout:

T : liquid H_2 target

M : spectrometer magnet

CH1-CH6 : multiwire proportional chambers

H1/H2,PR1/PR2 : trigger scintillation hodoscopes

C_1-C_4 : threshold Čerenkov counters

Fig. 2 : Differential cross-section of $\pi^- p$ elastic scattering.
Data at 20 and 30 GeV/c from this experiment.
Data at 6.2 GeV/c from ref. 3, 9.71, 9.84 GeV/c ref. 2,
22.6 GeV/c ref. 1.

Fig. 3 : Differential cross-section of $\pi^+ p$ elastic scattering.
Data at 20 GeV/c from this experiment, at 10 GeV/c from ref. 5.

Fig. 4 : Differential cross-section of $K^- p$ elastic scattering.
Data at 20 GeV/c from this experiment, at 6.2 GeV/c from ref. 3.

Fig. 5 : Energy dependence of the $\pi^- p \to \pi^- p$ differential cross-section as a function of $\cos \theta_{cm}$ for $19 < s < 57$ GeV^2 .
The cross-section is parametrized, at fixed $\cos \theta_{cm}$, as $\frac{d\sigma}{dt} = as^{-n}$. Plotted is the value of n .

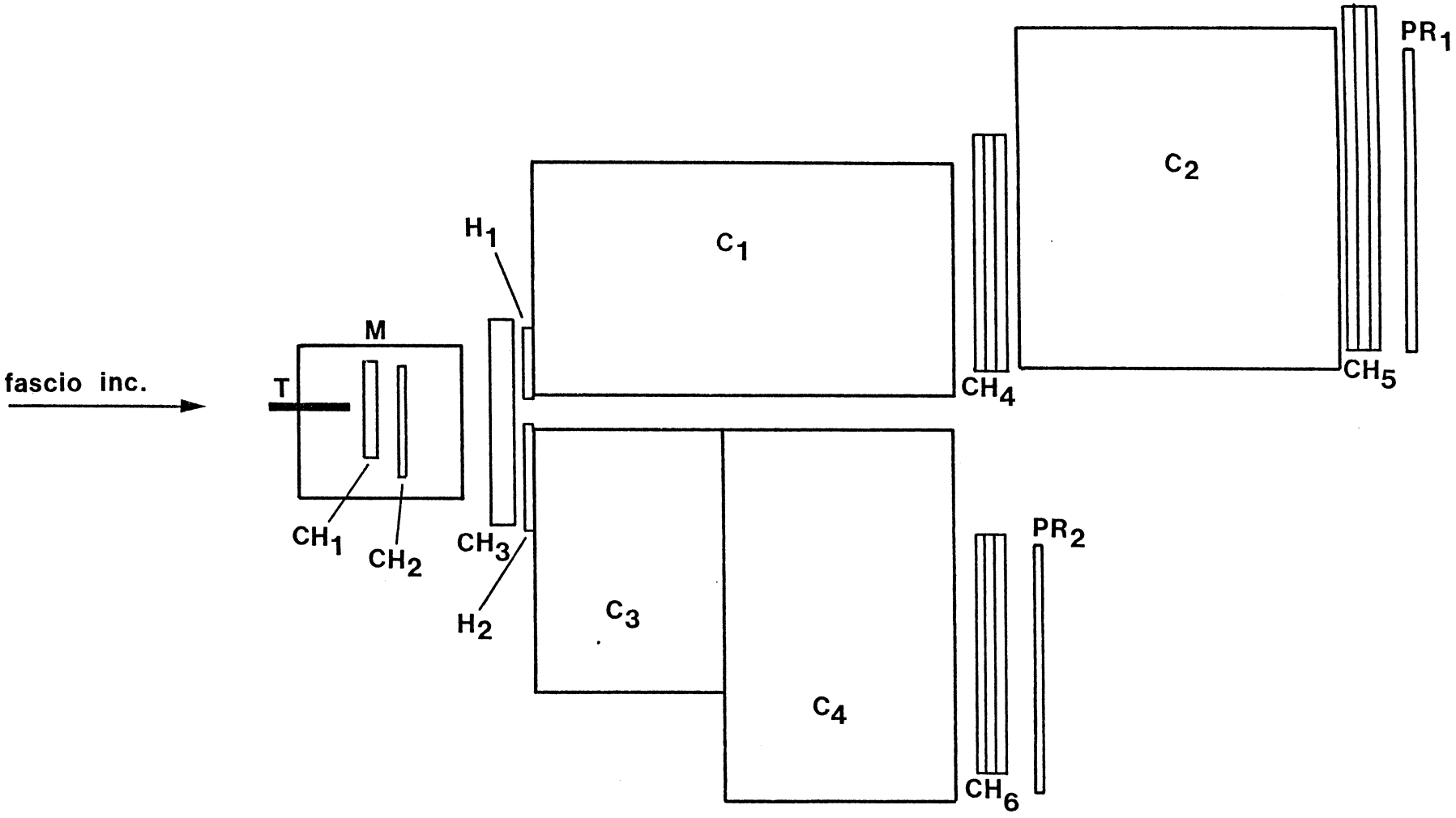

Fig. 1

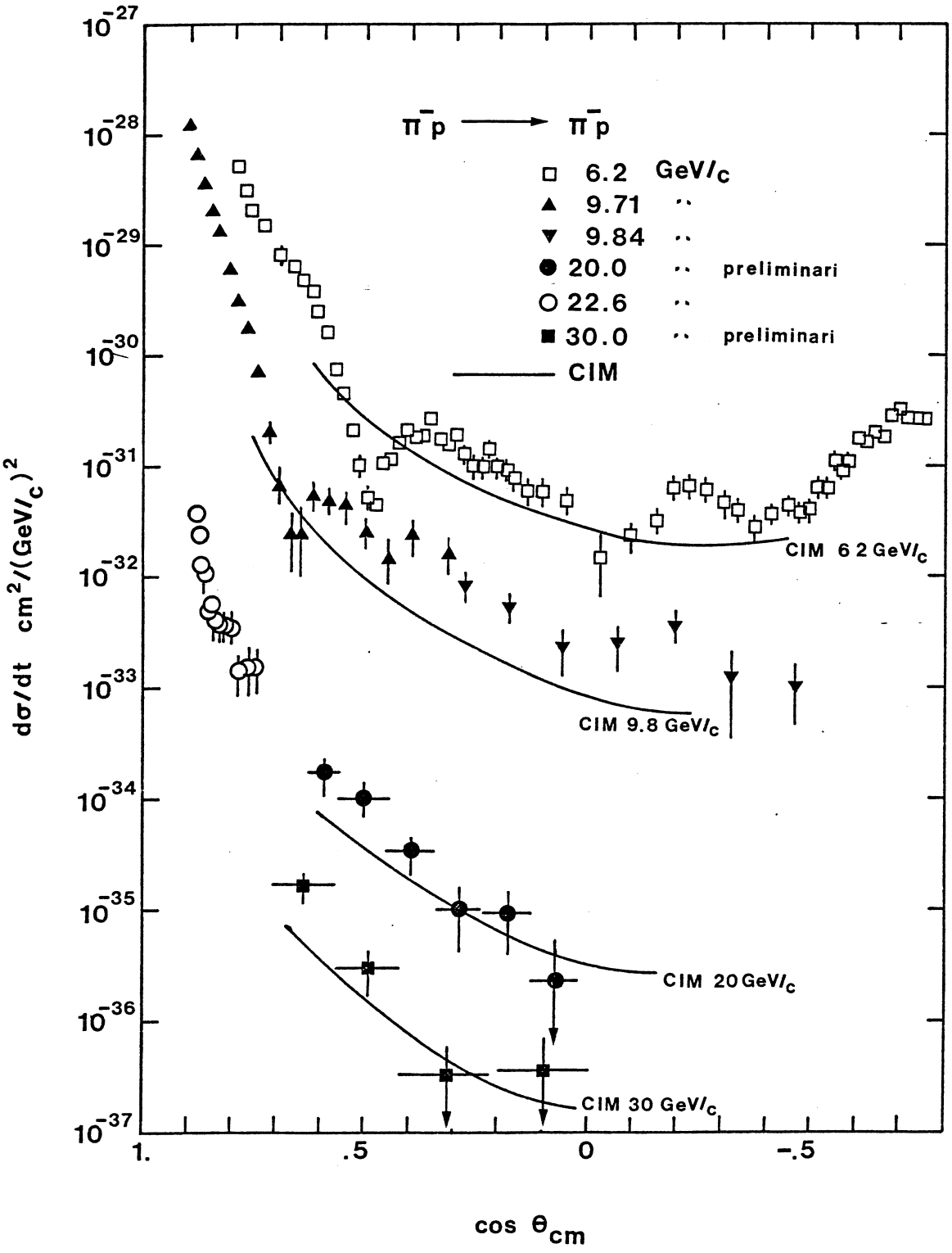
$\pi^- p \longrightarrow \pi^- p$
6.2 GeV/c
9.71 ··
9.84 ··
20.0 ·· preliminari
22.6 ··
30.0 ·· preliminari
CIM
CIM 6.2 GeV/c
CIM 9.8 GeV/c
CIM 20 GeV/c
CIM 30 GeV/c
$d\sigma/dt$ cm^2/(GeV/c)^2
cos θ_{cm}
10^{-27}
10^{-28}
10^{-29}
10^{-30}
10^{-31}
10^{-32}
10^{-33}
10^{-34}
10^{-35}
10^{-36}
10^{-37}
1.
.5
0
-.5

Fig. 2

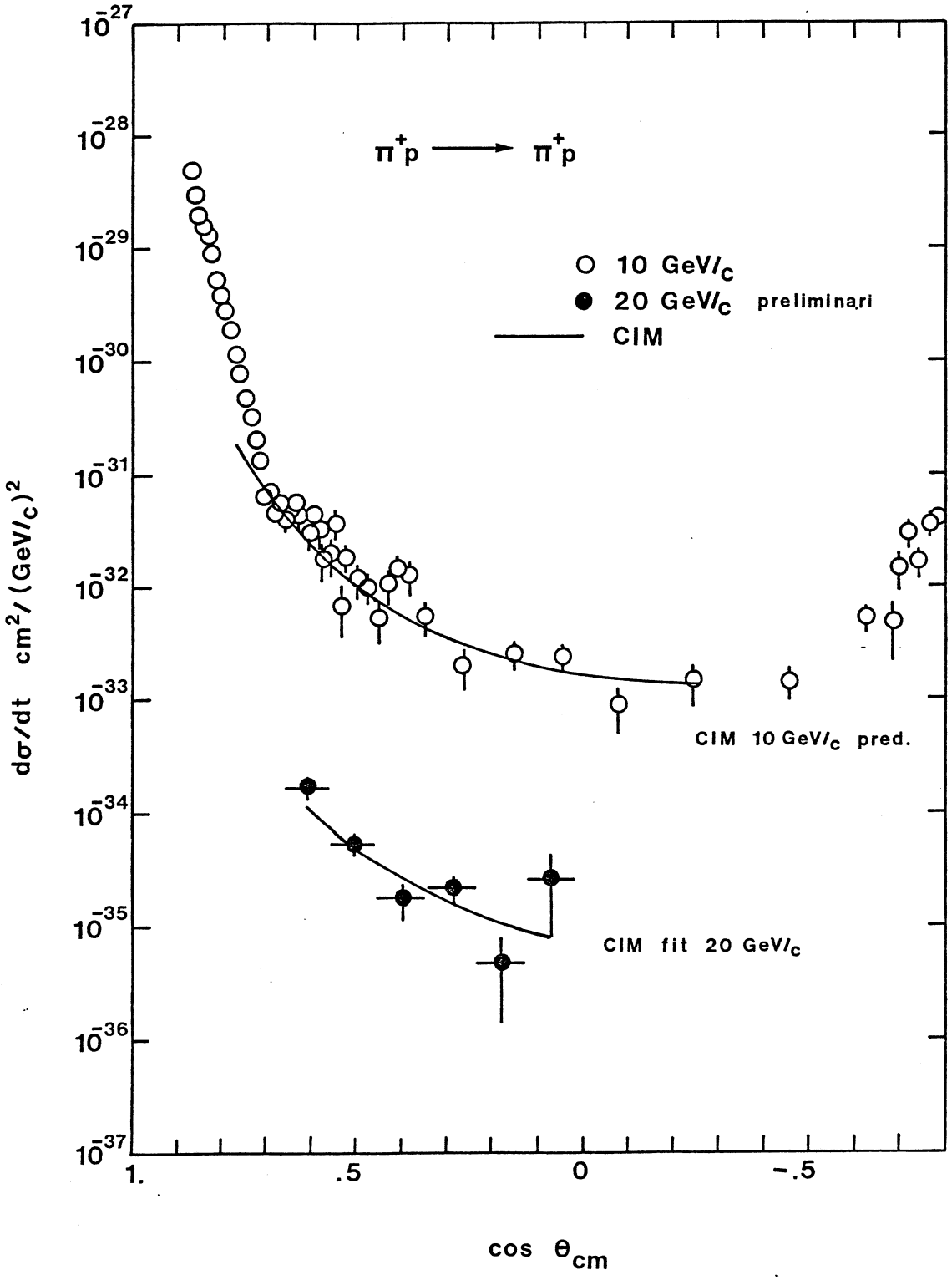
$\pi^+ p \longrightarrow \pi^+ p$
10 GeV/c
20 GeV/c preliminari
CIM
CIM 10 GeV/c pred.
CIM fit 20 GeV/c
$d\sigma/dt$ cm^2/(GeV/c)^2
10^{-27}
10^{-28}
10^{-29}
10^{-30}
10^{-31}
10^{-32}
10^{-33}
10^{-34}
10^{-35}
10^{-36}
10^{-37}
1.
.5
0
-.5
cos θ_{cm}

Fig. 3

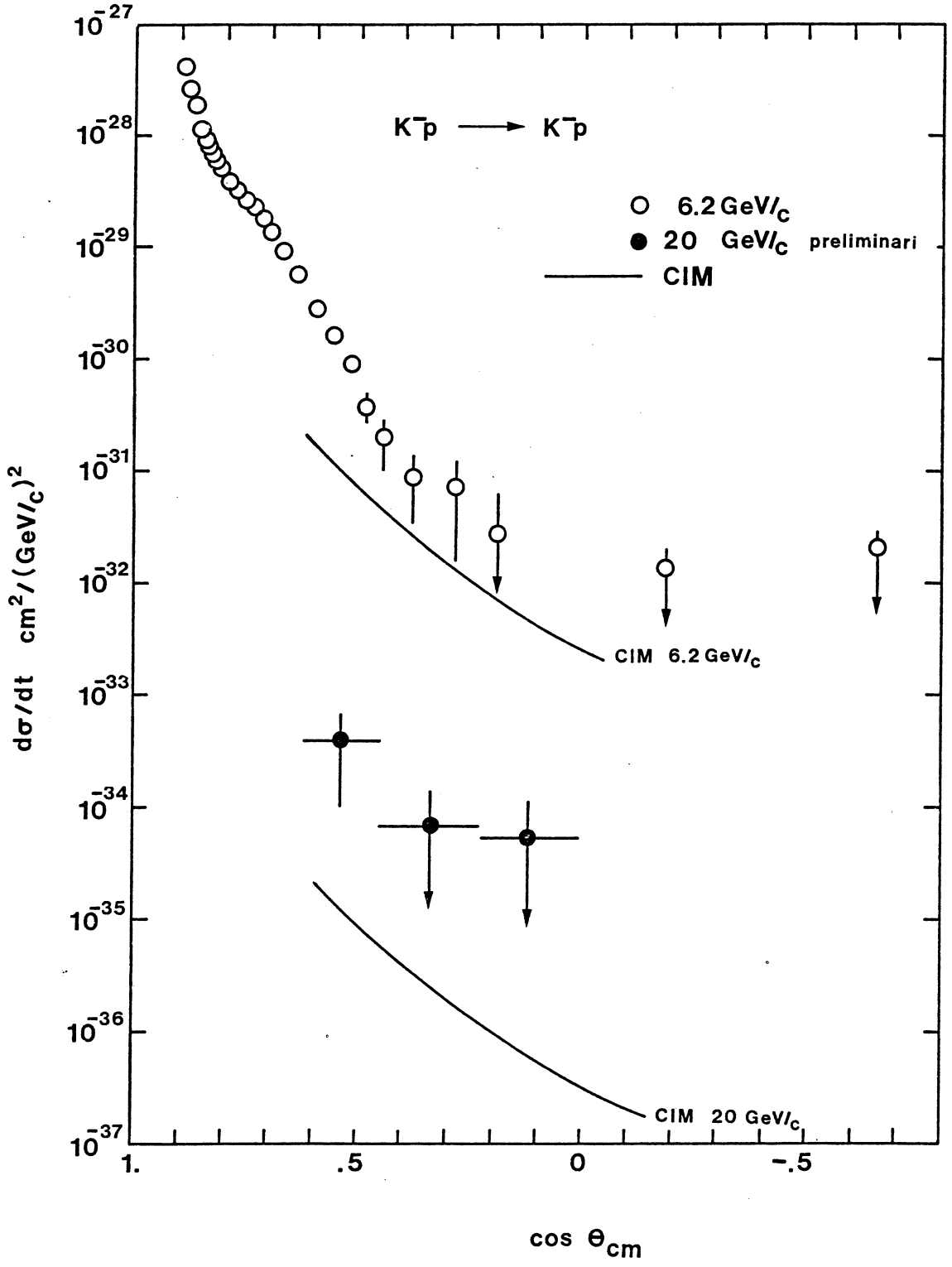
$K^-p \longrightarrow K^-p$
6.2 GeV/c
20 GeV/c preliminari
CIM
CIM 6.2 GeV/c
CIM 20 GeV/c
$d\sigma/dt$ cm^2/(GeV/c)^2
cos θ_{cm}
1.
.5
0
-.5

Fig. 4

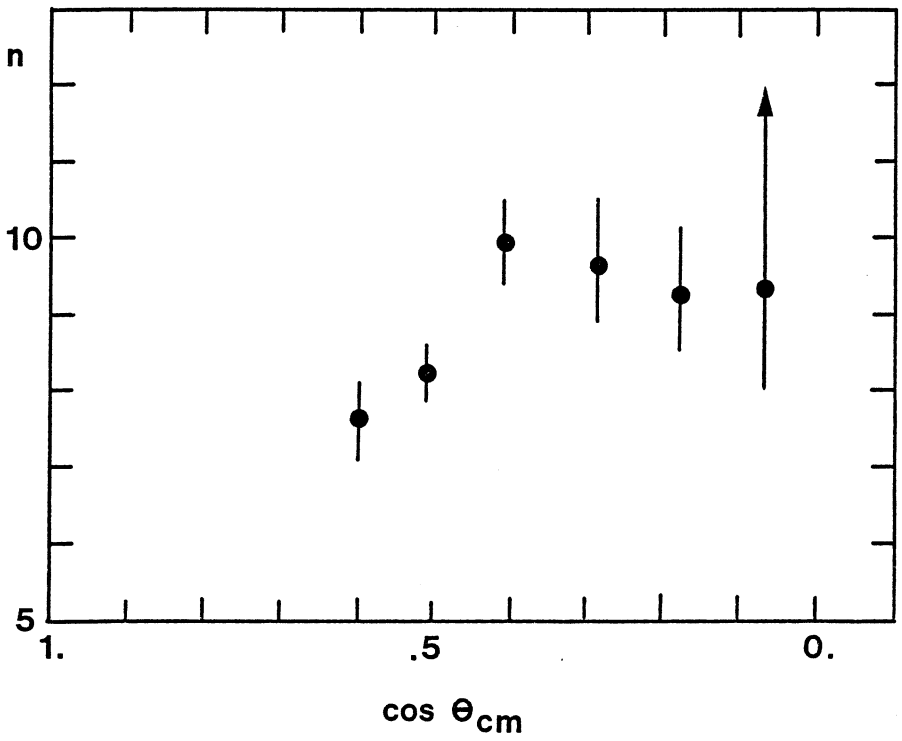

Fig. 5